Journal of Oceanography, Vol. 66, pp. 719 to 730, 2010

Specific Absorption Coefficient and Phytoplankton Community Structure in the Southern Region of the California Current during January 2002

EDUARDO MILLÁN-NÚÑEZ[1]* and ROBERTO MILLÁN-NÚÑEZ[2]

[1]*Centro de Investigación Científica y de Educación Superior de Ensenada, Ecología Marina, Carretera Ensenada-Tijuana No. 3918 Fraccionamiento Zona Playitas Ensenada, B.C., C.P. 22860, México*
[2]*Universidad Autónoma de Baja California, Facultad de Ciencias Marinas, Km 103 carretera Tijuana-Ensenada, Apartado Postal #453, Ensenada, B.C., C.P. 22880, México*

(Received 23 February 2010; in revised form 4 July 2010; accepted 19 August 2010)

Measurements of the specific absorption coefficients of phytoplankton (a^*_{ph}) are currently required to estimate primary productivity at regional to global scales using satellite imagery. The variability in a^*_{ph} and phytoplankton size fraction was determined during January 2002 in the southern region of the California Current. Median values of a^*_{ph} at 440 nm and 674 nm were 0.061 and 0.028 m^2 (mg Chl-*a*)$^{-1}$ and significant variability was found between inshore and offshore stations. A decrease of a^*_{ph} is associated with increased phytoplankton abundance and larger species. The a^*_{ph} tends to be high when the photoprotector zeaxanthin is present in elevated concentrations and phytoplankton abundance lower. The nano-microphytoplankton (>5 μm) community consisted of 28 diatom and 15 dinoflagellate genera with mean abundance values of 2.8 and 1.6 × 10^3 cells l^{-1}, respectively. The picophytoplankton (<5 μm) community consisted of *Prochlorococcus* sp. (mean 8.2 × 10^6 cells l^{-1}) and *Synechococcus* sp. (mean 19.5 × 10^6 cells l^{-1}), as well as a mixture of picoeukaryotes (mean 8.6 × 10^6 cells l^{-1}). The contributions of nano-microphytoplankton and picophytoplankton to the total biomass (μg C l^{-1}) were 46% and 54%, respectively. This study showed that picophytoplankton cells increased 2.5 times up during January 2002 compared with the previous year. It was concluded that the waning of La Niña conditions had a clear effect on the pelagic ecosystem in January 2002 and that the higher microphytoplankton abundance in the California Current was dominated by local and regional seasonal processes.

Keywords:
· Specific absorption,
· phytoplankton,
· flow cytometry,
· HPLC-pigments,
· California Current.

1. Introduction

Changes in phytoplankton species composition are a central feature of marine ecosystem dynamics. The description and prediction of these changes are important goals in many oceanographic fields. In recent years, great efforts have been made to understand how phytoplankton species composition can affect ocean-color optical properties (Morel, 1997; Stuart *et al*., 1998). Light absorption by phytoplankton pigments is a key parameter in wavelength-resolved bio-optical models for characterizing regional maps of primary productivity using remotely-sensed data. Variability in the optical properties of phytoplankton may result from changes in the community structure and in cell size distributions. Several investigations have attempted to improve the different bio-optical models to better describe/capture the regional phytoplankton ecology (Kiefer and Mitchell, 1983; Sathyendranath *et al*., 1995; Behrenfeld and Falkowski, 1997). The specific absorption coefficient (a^*_{ph}) is an essential parameter because it constitutes the link between phytoplankton biomass and light absorption by pigments. The variability in a^*_{ph} has previously been described by Yentsch and Phinney (1989), Nelson *et al*. (1993), Sosik and Mitchell (1995), Millán-Núñez *et al*. (2004), Wu *et al*. (2007), and Barocio-León *et al*. (2008) and they have

* Corresponding author. E-mail: emillan@cicese.mx
Present address: CICESE, División de Oceanología, P.O. Box 434844, San Diego, CA 92143-4844, U.S.A.

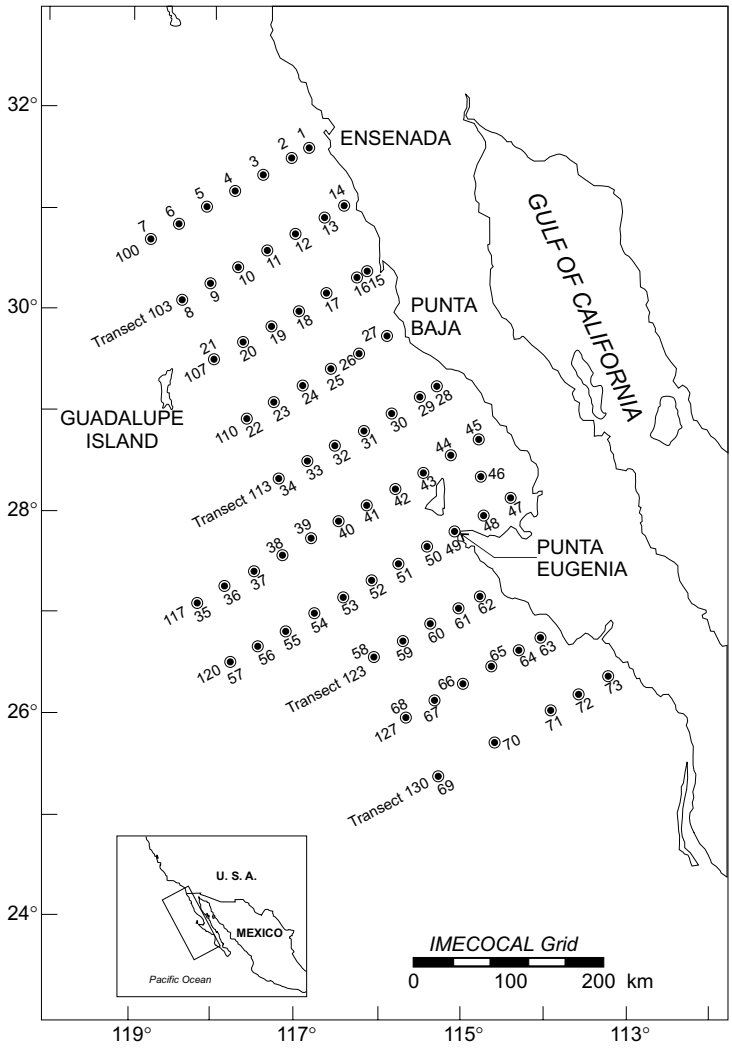

Fig. 1. Study area and location of stations sampled during the January 2002 cruise off Baja California. Samples were taken at 10 m depth.

attributed this variability to the relation between photosynthetic and photoprotective carotenoids, blue-red ratio of phytoplankton absorption, and sizes of phytoplankton species. The goal of this study is to understand the variability in a^*_{ph} relative to changes in the phytoplankton community structure during January 2002 in the southern region of the California Current.

2. Materials and Methods

2.1 Sampling and storage

The Mexican California Current research program (IMECOCAL, acronym for Investigaciones Mexicanas de la Corriente de California) was designed to occupy the historical CalCOFI (California Cooperative Oceanic Fisheries Investigations (CalCOFI) transects in Mexican waters. Figure 1 shows the location of the 10 transects and 73 hydrographic stations (37 km between stations and 74 km between transects); data taken at each station include conductivity-temperature-depth (CTD/rosette) casts to 1000 m water depth permitting. Samples were collected in coastal/oceanic waters off Baja California between 19 January and 06 February 2002 at a depth of 10 m with 5-litre polyethylene Niskin bottles using Tygon tubing. Particulate matter was filtered through Whatman GF/F filters for the analysis of spectral absorption coefficients and phytoplankton pigment. Samples for microscope analysis were stored in 250 ml dark bottles and preserved with formalin-borate (0.4% final concentration). Seawater samples of 4 ml were preserved with glutaraldehyde (0.1% final concentration) and stored in liquid nitrogen until analysis by flow cytometry.

Table 1. Specific absorption coefficient by phytoplankton (a^*_{ph}) at 440 nm and 674 nm (m^2(mg Chl-*a*)$^{-1}$, blue/red ratio (b/r) (a_{ph} 440/a_{ph} 674) from 10 metre samples collected during January 2002. Trans. = transects showing a subset of the original CalCOFI grid.

Trans.	Sta.	Date/time (day/gmt)	a^*_{ph} (440 nm)	a^*_{ph} (674 nm)	Ratio (b/r)	Trans.	Sta.	Date/time (day/gmt)	a^*_{ph} (440 nm)	a^*_{ph} (674 nm)	Ratio (b/r)
100.30	1	19/01/20:18	0.1265	0.0512	2.47	117.65	38	29/01/06:02	0.0379	0.0088	4.33
100.35	2	20/01/01:47	0.1000	0.0325	3.07	117.60	39	29/01/11:43	0.0665	0.0267	2.48
100.40	3	20/01/06:15	0.0783	0.0289	2.71	117.55	40	29/01/18:46	0.0694	0.0284	2.43
100.45	4	20/01/11:18	0.0779	0.0304	2.56	117.50	41	29/01/21:86	0.0650	0.0264	2.46
100.50	5	21/01/15:27	0.0950	0.0309	3.07	117.45	42	30/01/04:55			
100.55	6	21/01/01:50	0.0847	0.0249	3.39	117.40	43	30/01/10:12	0.0539	0.0234	2.30
100.60	7	21/01/08:36	0.0863	0.0380	2.17	117.35	44	30/01/15:09			
103.60	8	21/01/15:36	0.0870	0.0399	2.22	117.30	45	30/01/19:19			
103.55	9	21/01/21:02	0.0593	0.0268	2.21	119.33	46	31/01/00:14			
103.50	10	22/01/03:33	0.0985	0.0293	3.23	120.30	47	01/02/07:00	0.0610	0.0294	2.06
103.45	11	22/01/08:15	0.0609	0.0249	2.44	120.35	48	01/02/10:40	0.0688	0.0310	2.21
103.40	12	22/01/13:35	0.0515	0.0258	1.99	120.40	49	01/02/13:07	0.0640	0.0300	2.13
103.35	13	22/01/18:41	0.0244	0.0081	3.00	120.45	50	01/02/17:42	0.0604	0.0290	2.08
103.30	14	22/01/22:20	0.0567	0.0299	1.89	120.50	51	01/02/23:50	0.0503	0.0224	2.23
107.32	15	23/01/18:03	0.0641	0.0307	2.08	120.55	52	02/02/04:48	0.0581	0.0293	1.98
107.35	16	23/01/21:20	0.0606	0.0317	2.30	120.60	53	02/02/08:45	0.0653	0.0294	2.21
107.40	17	24/01/03:41	0.0694	0.0321	2.16	120.65	54	02/02/13:43	0.1041	0.0469	2.21
107.45	18	24/01/08:58	0.0590	0.0280	2.10	120.70	55	02/02/17:55	0.0969	0.0401	2.41
107.50	19	24/01/14:01	0.0367	0.0180	2.03	120.75	56	03/02/00:46	0.0382	0.0129	2.94
107.55	20	24/01/20:34	0.0657	0.0254	2.58	120.80	57	03/02/04:15	0.0629	0.0259	2.42
107.60	21	24/01/03:37	0.0869	0.0258	3.36	123.60	58	03/02/17:05	0.0267	0.0129	2.06
110.60	22	25/01/11:05	0.0653	0.0239	2.74	123.55	59	03/02/23:30	0.0668	0.0377	1.77
110.55	23	25/01/15:59	0.0495	0.0216	2.28	123.50	60	04/02/02:47	0.0680	0.0297	2.28
110.50	24	25/01/21:50	0.0551	0.0173	2.22	123.45	61	04/02/06:43	0.0442	0.0190	1.91
110.45	25	26/01/07:33				123.42	62	04/02/09:46	0.0957	0.0509	1.88
110.40	26	25/01/07:26	0.0588	0.0269	1.71	127.35	63	04/02/16:58	0.0727	0.0340	2.13
110.35	27	26/01/12:26	0.0580	0.0291	1.99	127.40	64	04/02/21:39	0.0473	0.0256	1.84
113.30	28	26/01/19:45	0.0561	0.0223	2.50	127.45	65	04/02/01:19	0.0605	0.0280	2.16
113.35	29	26/01/23:20	0.0602	0.0293	2.04	127.50	66	04/02/05:27	0.0234	0.0061	2.45
113.40	30	27/01/04:19	0.0709	0.0294	2.40	127.55	67	05/02/09:08	0.0524	0.0281	1.86
113.45	31	27/01/09:02	0.0653	0.0285	2.28	127.60	68	05/02/12:43	0.0406	0.0228	1.77
113.50	32	27/01/13:15	0.0562	0.0215	2.61	130.60	69	05/02/19:51	0.0341	0.0144	2.36
113.55	33	27/01/17:40				130.50	70	06/02/06:10	0.0536	0.0314	1.70
113.60	34	28/01/00:02	0.0663	0.0290	2.27	130.40	71	06/02/12:01	0.0515	0.0285	1.80
117.80	35	28/01/14:22				130.35	72	06/02/16:33	0.0264	0.0059	4.45
117.75	36	28/01/17:55	0.0551	0.0227	2.41	130.30	73	06/02/20:08	0.1240	0.0638	2.41
117.70	37	29/01/00:46	0.0599	0.0263	2.28						

2.2 Absorption coefficient of phytoplankton

Samples for light absorption by phytoplankton were filtered onto Whatman GF/F glass microfiber filters (25 mm, 0.7 μm). Sample filters were put into tissue capsules (Fisher HistoPrep) and then stored in liquid nitrogen for a maximum of one month until analysis. Blank filters were saturated with seawater through 0.2-μm Nuclepore filters. Absorption of sample and blank filters was measured on a Perkin-Elmer Lambda 10 spectrophotometer with integrating sphere, following the procedure proposed by Mitchell (1990) and Cleveland and Weidemann (1993). Sample absorption was measured between 400 and 750 nm at 1-nm resolution, and repeated after rinsing the filters twice with warm methanol (Kishino *et al.*, 1985) for 15 minutes. The absorption spectra were corrected for two factors: baseline from blank filters and path-length amplification (β) by adjusting the optical density of the filtered samples ($OD_{fil}(\lambda)$) to the optical density of samples in suspension ($OD_{sus}(\lambda)$) (Eq. (1)), which were previously determined using the spectrophotometer. Phytoplankton pigment absorption ($a_{ph}(\lambda)$) was determined as the difference between total particulate matter absorption ($a_p(\lambda)$) and non-pigmented or detritus material absorption ($a_{det}(\lambda)$) (Eq. (2)). The specific absorption coefficient of

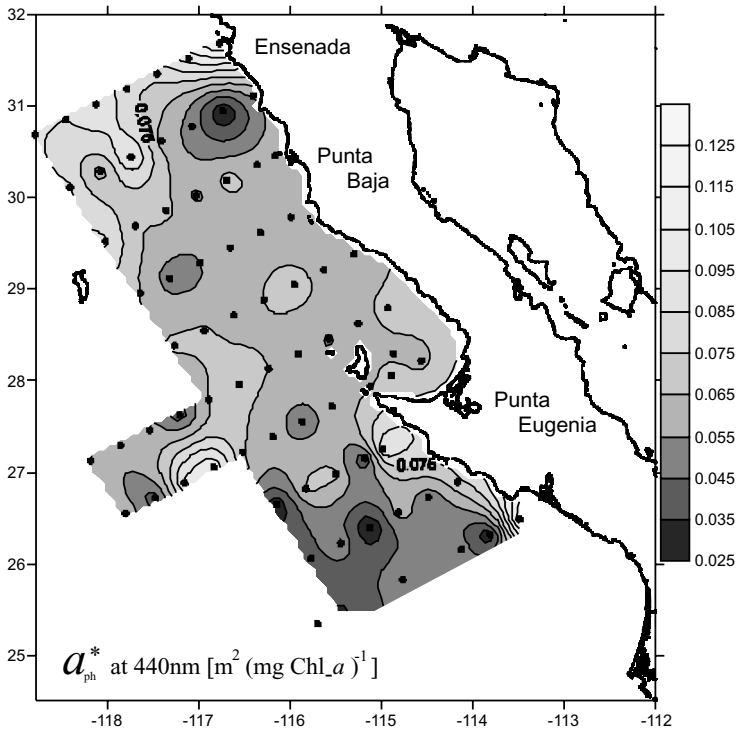

Fig. 2. Spatial distribution of the specific absorption coefficient (a^*_{ph} at 440 nm) (m^2(mg Chl-*a*)$^{-1}$) at 10 m depth during January 2002.

phytoplankton (a^*_{ph}) was obtained by normalizing the phytoplankton absorption data (m^{-1}) by the concentration of chlorophyll-*a* (Chl-*a*, mg m^{-3}) measured by high-performance liquid chromatography (HPLC) (Eq. (3)):

$$OD_{sus} = 0.368OD_{filt} + 0.4068(OD_{filt})^2 \quad (1)$$

$$a_{ph}(\lambda) = a_p(\lambda) - a_{det}(\lambda) \quad (2)$$

$$a^*_{ph}(\lambda) = a_{ph}(\lambda)/\text{Chl-}a. \quad (3)$$

2.3 Microscope observation of phytoplankton

Within two months of sampling, 50 ml of water were allowed to settle in a composite chamber and examined using the inverted microscope technique (Utermöhl, 1958). Diatoms and dinoflagellates (>5 μm) were classified to the lowest possible taxonomic level, and identified based on Licea *et al*. (1996) and Moreno *et al*. (1997). Only in the case of diatoms, the cells (length and width) were measured using a micrometer. These measurements of the nano-microphytoplankton size fractions were converted to biovolume assuming the steriometric shapes suggested by Strathmann (1967) and Edler (1979). The equation proposed by Verity *et al*. (1992) was then used to convert volume to carbon concentration. For *Synechococcus* sp., picoeukaryotes, and *Prochlorococcus* sp., mean cell biovolumes of 0.52, 3.05, and 0.27 μm^3, respectively, were assumed.

2.4 Flow cytometry

Samples were processed through a FACScan flow cytometer (Becton-Dickinson) with an air-cooled argon (488 nm) laser at high flow rate (ca. 60 μl min^{-1}) for 5 min or until 10^6 events had been recorded. Data were acquired by triggering on chlorophyll fluorescence (FL3) in log mode. As an internal standard, we added 10 μl per 600 μl sample of a 10^5 ml^{-1} solution of yellow-green 0.92 μm diameter Polysciences latex beads. *Synechococcus* sp. cells were detected by the orange fluorescence signature of phycoerythrin (FL2) versus red chlorophyll fluorescence (FL3). *Prochlorococcus* sp. were distinguished by a lower FL3 signal and no FL2 signal. Autotrophic picoeukaryotes had higher FL3 and scatter signals and low or no FL2 signal.

2.5 HPLC analysis of pigments

Chlorophylls and carotenoids were separated at the Center for Hydro-Optics and Remote Sensing (CHORS) at San Diego State University, using the Wright *et al*. (1991) method, which separates the major pigment compounds found in phytoplankton. An internal pigment standard canthaxanthin was added to the 90% acetone

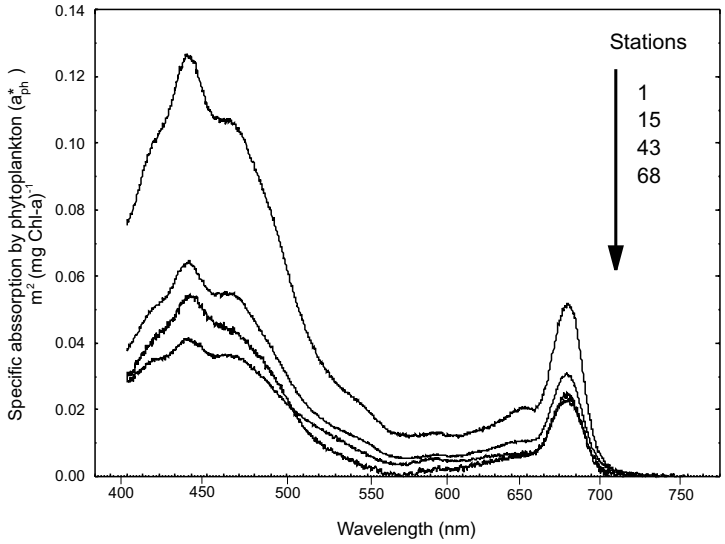

Fig. 3. Spectral magnitude of specific absorption by phytoplankton at 10 m depth during January 2002. The numbers to the right of the arrow show the position sequence of the stations.

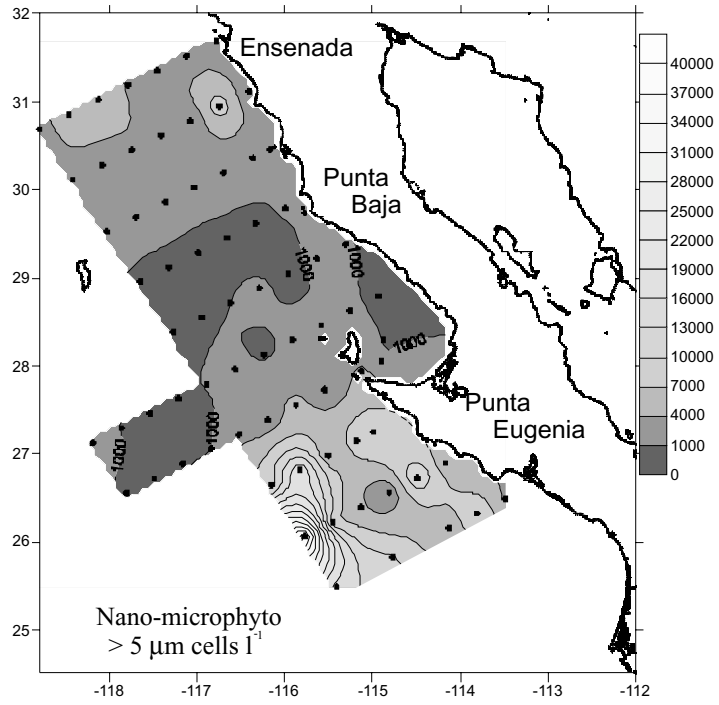

Fig. 4. Spatial distribution of nano-microphytoplankton (>5 μm cells l^{-1}) at 10 m depth during January 2002. Abundance estimated by inverted microscopy.

sample to correct for volume changes during the extraction process. Pigment peaks were detected by a two-channel absorption detector (436 and 450 nm), a scanning diode array absorption detector (190 to 800 nm at 1 nm resolution) and a fluorescence detector for degradation products. Although the absorption peaks for monovinyl Chl-*a* and divinyl Chl-*a* co-elute using this method, each compound absorbs differently at 436 and 450 nm and it

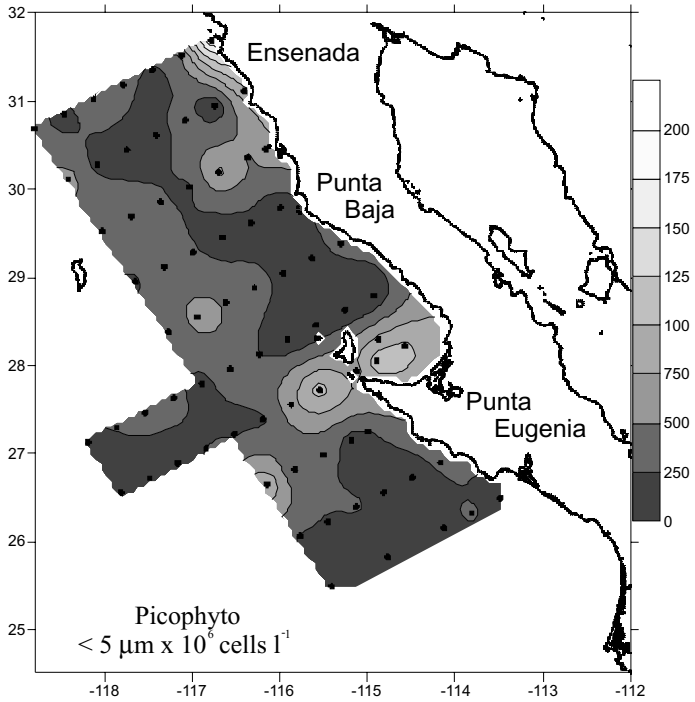

Fig. 5. Spatial distribution of picophytoplankton (<5 μm $\times$ 10^6 cells l^{-1}) (prochlorophytes, picoeukaryotes, and cyanobacteria) at 10 m depth during January 2002. Abundance estimated by flow cytometry.

is therefore possible to correct for divinyl Chl-*a* contamination by monitoring changes in this ratio as a function of changes in the divinyl percentages (Latasa *et al*., 1996).

3. Results

3.1 Specific absorption coefficient of phytoplankton

At 10 m depth during the survey period, a^*_{ph} at 440 -nm ($a^*_{ph}(440)$) varied between 0.024 and 0.126 m^2 (mg Chl-*a*)$^{-1}$, while a^*_{ph} at 674 nm ($a^*_{ph}(674)$) varied between 0.008 and 0.065 (Table 1). The minimum values of $a^*_{ph}(440)$ were found at station 13, located to the south of Ensenada, and at stations 58, 68, and 69 off Punta Eugenia; this parameter is not homogeneous, and it presents some small areas with higher and lower values (Fig. 2). The magnitude of the spectral absorption curves showed greater variability in the blue band (440 nm) than in the red band (674 nm) (Fig. 3). The blue red peak ratio (a_{ph} 440 nm/a_{ph} 674 nm) ranged from 1.70 to 4.45 (Table 1).

3.2 Phytoplankton community structure

Abundances of nano-microphytoplankton (>5 μm) were highest at the farshore stations off Punta Eugenia, on transects 123 and 127 (Fig. 4). Taxonomic analyses revealed a total of 28 diatom and 15 dinoflagellate genera. The most common diatoms were *Nitzschia* spp., *Thalassionema* sp., and *Chaetoceros* spp., while the most common dinoflagellates were *Gymnodinium* spp., *Gyrodinium* spp., and *Prorocentrum* sp. High diatom abundances of ~37.8 $\times$ 10^3 cells l^{-1} were observed at stations 59, 68, and 69. Dinoflagellate abundances ranged from 0.2 to 25 $\times$ 10^3 cells l^{-1} off Baja California, with higher values at stations 11 and 13 in the northern area, and at station 64 to the south.

The abundance of picophytoplankton (<5 μm) was ~50 $\times$ 10^6 cells l^{-1} in the study area, except at stations 1, 2, 47, 48, 50, 51, and 58 where values were above 50 $\times$ 10^6 and up to 195 $\times$ 10^6 cells l^{-1} (Fig. 5). The most abundant organism was *Synechococcus* sp. with values ranging from 0.02 to 132 $\times$ 10^6 cells l^{-1}, followed by picoeukaryotes with 0.2 to 60 $\times$ 10^6 cells l^{-1}, while *Prochlorococcus* sp. ranged from not detected to 57 $\times$ 10^6 cells l^{-1}. The contributions of the size-fractionated biomass to total phytoplankton (μg C l^{-1}) were 36% for microphytoplankton, 32% for picoeukaryotes, 16% for *Synechococcus* sp., 10% for nanophytoplankton, and 6% for *Prochlorococcus* sp. (Fig. 6). The smaller cells (picophytoplankton) made up the dominant size fraction, contributing 54% of the total phytoplankton biomass.

3.3 Pigments

Zeaxanthin is a characteristic pigment of *Synechococcus* sp. while divinyl Chl-*a* is a unique pig-

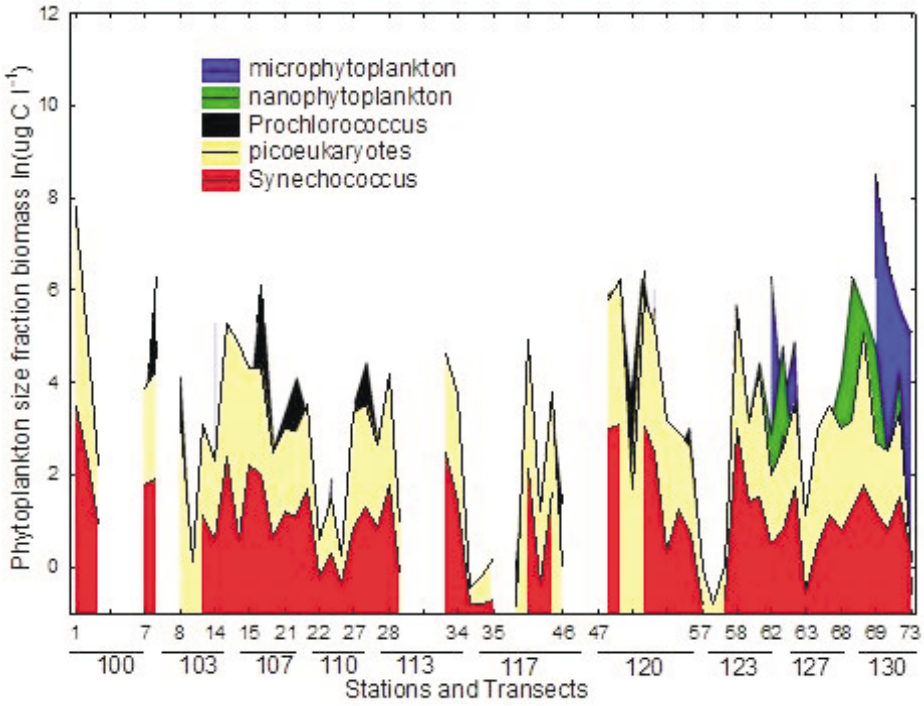

Fig. 6. Contribution of each phytoplankton group to size-fractioned biomass ln (μg C l^{-1}), at 10 m depth during January 2002: microphytoplankton, nanophytoplankton, *Prochlorococcus* sp., picoeukaryotes, and *Synechococcus* sp.

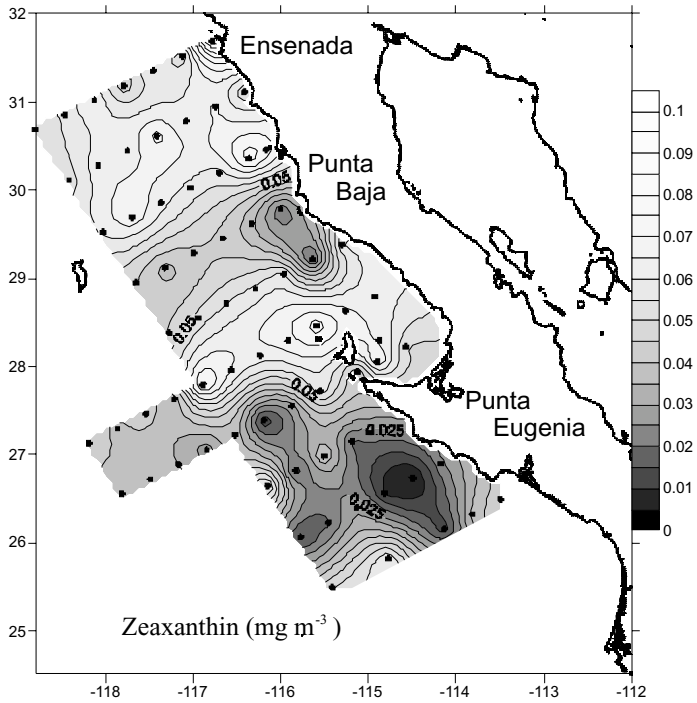

Fig. 7. Spatial distribution of zeaxanthin (mg m^{-3}) at 10 m depth during January 2002. Pigments concentration estimated by HPLC.

Table 2. Pigment concentrations (mg m^{-3}). Chlorophyll-*a* (Chl-*a*), zeaxanthin (Zea), divinyl chlorophyll-*a* (DV Chl-*a*), from 10 m samples collected during January 2002.

Sta.	Chl-*a*	Zea	DV Chl-*a*	Sta.	Chl-*a*	Zea	DV Chl-*a*
1	1.328	0.099	0.013	38	0.140	0.036	0.067
2	0.377	0.052	0.054	39	0.513	0.077	0.112
3	0.281	0.060	0.111	40	0.762	0.065	0.144
4	0.197	0.046	0.078	41	0.871	0.063	0.067
5	0.219	0.065	0.094	42			
6	0.195	0.056	0.069	43	0.650	0.078	0.183
7	0.182	0.051	0.090	44			
8	0.270	0.052	0.091	45			
9	0.194	0.063	0.087	46			
10	0.160	0.061	0.080	47	0.894	0.050	0.023
11	0.291	0.072	0.086	48	0.964	0.071	0.074
12	0.256	0.060	0.097	49	0.543	0.040	0.016
13	0.287	0.066	0.102	50	1.323	0.059	0.054
14	1.569	0.050	0.077	51	1.315	0.028	0.023
15	2.143	0.073	0.050	52	0.688	0.011	0.012
16	0.578	0.078	0.150	53	0.714	0.039	0.050
17	0.497	0.058	0.089	54	0.448	0.027	0.063
18	0.452			55	0.165	0.035	0.075
19	0.431			56	0.174	0.039	0.089
20	0.405	0.069	0.134	57	0.142	0.037	0.070
21	0.296	0.061	0.085	58	1.336	0.063	0.027
22	0.181	0.045	0.077	59	0.579	0.017	0.001
23	0.257	0.038	0.076	60	0.640	0.041	0.070
24	0.156	0.044	0.073	61	0.703	0.019	0.029
25				62	0.614	0.024	0.046
26	0.376	0.036	0.053	63	0.465	0.024	0.023
27	0.364	0.021	0.042	64	0.790	0.004	0.001
28	0.637	0.060	0.085	65	0.561	0.009	0.018
29	0.296	0.017	0.029	66	0.533	0.030	0.034
30	0.580	0.057	0.098	67	0.818	0.019	0.027
31	0.711	0.056	0.125	68	1.143	0.014	0.010
32	0.736			69	0.970	0.050	0.027
33				70	1.347	0.016	0.016
34	0.786	0.045	0.077	71	1.290	0.012	0.019
35	0.122	0.043	0.062	72	0.650	0.037	0.044
36	0.151	0.039	0.079	73	0.472	0.044	0.052
37	0.199	0.043	0.092				

ment of *Prochlorococcus* sp. Values greater than 0.03 mg m^{-3} were recorded for zeaxanthin in the northern part of the study area, above transect 117, except at nearshore stations off Punta Baja (Fig. 7, Table 2). The concentrations of Chl-*a* ranged from 0.14 to 2.14 mg m^{-3} (Table 2), and values higher than 0.90 mg m^{-3} were observed off Ensenada and Punta Eugenia, which have been reported to be upwelling areas (Álvarez-Borrego and Álvarez-Borrego, 1982; Durazo *et al*., 2005). High Chl-*a* values were also found in areas with low divinyl Chl-*a* concentrations. Overall, both zeaxanthin and divinyl Chl-*a* showed the same tendency of variation and a good correlation ($r = 0.76$, $p < 0.05$) (Fig. 8).

4. Discussion

The physical oceanographic conditions of the California Current during this period were characterized by Schwing *et al*. (2002). These authors concluded, based on the Multivariate El Niño/Southern Oscillation (ENSO) Index (MEI; Wolter and Timlin, 1998) and Pacific Decadal Oscillation (PDO; Mantua *et al*., 1997) that the winter of 2001–2002 marked the onset of warm upper-ocean thermal anomalies in the California Current system after the pattern of cool anomalies that had persisted for several years. Schwing *et al*.'s oceanographic evidence and the pelagic ecosystem response to interannual variability off Baja California reported by Gaxiola-Castro *et al*. (2008)

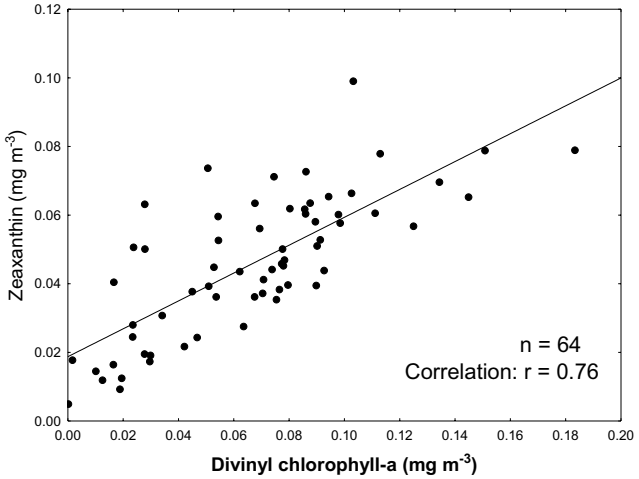

Fig. 8. Pigment (mg m^{-3}) correlation of zeaxanthin versus divinyl Chl-*a*. The line represents the tendency at 95% confidence between both variables at 10 m depth during January 2002.

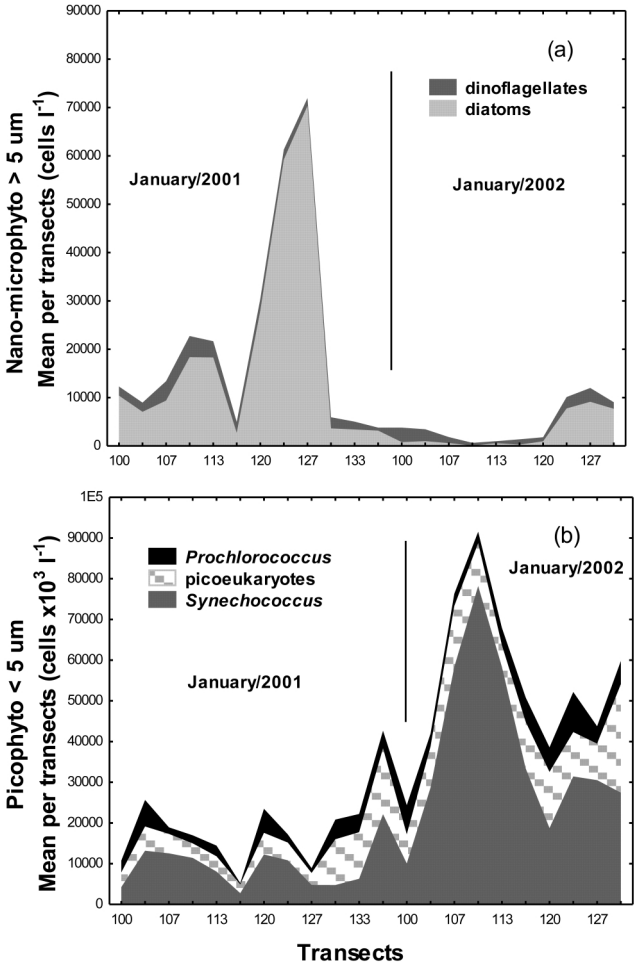

Fig. 9. Mean phytoplankton abundance per transect at 10 m depth during January 2001 and January 2002: (a) nano-microphytoplankton (diatoms and dinoflagellates), and (b) picophytoplankton (*Prochlorococcus*, *Synechococcus*, and picoeukaryotes).

support the findings of Millán-Núñez *et al*. (2004), who observed that in January 2001 the abundance of nano-microphytoplankton increased and that of picophytoplankton decreased in relation to each other. Compared with January 2001, our results for January 2002 showed an abundance of diatoms (mean of 2.8×10^3 cells l^{-1}, approximately 7 times less in respect to January 2001) and dinoflagellates (mean of 1.6×10^3 cells l^{-1}, decreased to 68% of the mean abundance of January 2001) (Fig. 9(a)), and a significant increase of picophytoplankton abundance approximately 2.5 times up in respect to January 2001 (Fig. 9(b)). This shift could be due to the oligotrophic warm ocean waters conditions at the end of the La Niña event. In accordance with the National Centers for Environmental Prediction (2002), these results suggest that the warming of upper ocean waters in the eastern equatorial Pacific in early 2002 was due to an oceanic Kelvin wave that propagated eastward from the central equatorial Pacific starting in mid-December. Samples collected off Punta Eugenia were characterized by higher diatom abundances, probably because of a strong frontal zone associated with high (~19°C) near-surface temperatures (Fig. 10). These thermal and saline fronts often recorded off Baja California (Roden, 1971) may provide the appropriate niches for the development of moderate phytoplankton concentrations in the region.

At station 57, which had the most oceanic water characteristics, the picophytoplankton was comprised of 29% *Synechococcus* sp., 27% picoeukaryotes, and 44% *Prochlorococcus* sp. These data show an increase of 28% and 22% for *Synechococcus* sp. and picoeukaryotes, respectively, and a decrease of 50% for *Prochlorococcus* sp. relative to those from January 2001 for the same station. Our values for *Prochlorococcus* sp. were lower than those reported by Blanchot *et al*. (2001) for the equatorial Pacific and by Gin *et al*. (2003) for the coastal waters of Singapore. Likewise, Goericke *et al*. (2000) reported *Prochlorococcus* sp. cell values of up to 160×10^6 cells l^{-1} at 10 m depth for the eastern tropical north Pacific in May 1997. However, these authors found that the highest abundances of *Prochlorococcus* sp. were located in the upper layers of the oxygen minimum zone or at the bottom of the euphotic zone. In this study, the highest value of *Prochlorococcus* sp. (~70×10^6 cells l^{-1}) was detected at station 43, corresponding to the highest concentration of divinyl Chl-*a* (0.183 mg m^{-3}, Table 2).

In general, the specific absorption coefficient was higher than that reported for January 2001 by Millán-

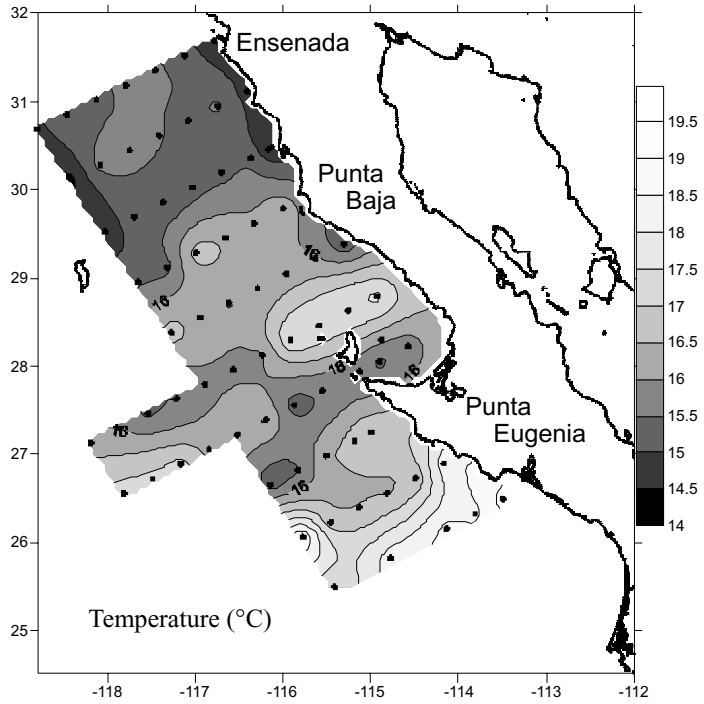

Fig. 10. Spatial distribution of temperature (°C) at 10 m depth during January 2002. Temperature estimated by CTD.

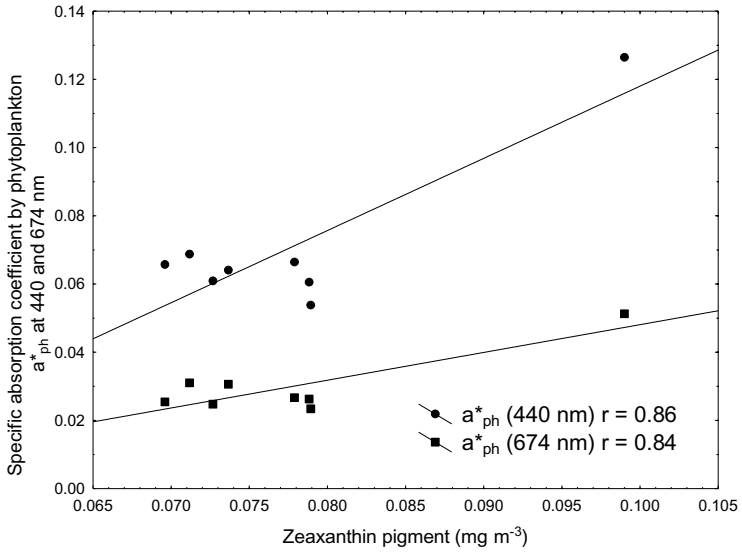

Fig. 11. Linear correlation between the specific absorption coefficient of phytoplankton (a^*_{ph} at 440 nm and 674 nm; m^2(mg Chl-*a*)$^{-1}$) and zeaxanthin (mg m^{-3}) for samples taken at 10m depth during January 2002. The line represents the tendency at 95% confidence between both variables.

Núñez *et al*. (2004) but lower for those reported for November 2002 by Barocio-León *et al*. (2006) as a consequence of changes in the oceanographic conditions after La Niña began to wane. In this study the blue/red peak ratios ranged from 1.70 to 4.45. These values are similar to those obtained by Sosik and Mitchell (1995) for the California Current and by Wu *et al*. (2007) for the northern South China Sea (1.9–3.9) during two cruise surveys in spring (May) 2001 and late autumn (November) 2002. According to these authors a blue/red ratio number greater

than 3.0 implies the predominance of picoprocaryotes in the phytoplankton community. When zeaxanthin is present in the ocean, we are artificially increasing a^*_{ph}, because, we normalized the phytoplankton absorption coefficient only by the Chl-*a* concentration. Likewise, we observed that a^*_{ph} (440 nm and 674 nm) shows a significant correlation when zeaxanthin concentration is higher than 0.070 mg m^{-3} (r = 0.86 and 0.84, $p < 0.05$, respectively) (Fig. 11). These results concur with those published by Staehr *et al*. (2004) and Hoepffner and Sathyendranath (1991), who explain that zeaxanthin absorbs strongly in the blue region and affects the variability of the spectral shape (Fig. 3). The increase in phytoplankton biomass and Chl-*a* pigment contributed significantly to the variability of a^*_{ph}; therefore, station samples with lower biomass and lower chlorophyll pigments had higher a^*_{ph} values and vice versa. These results are in accordance with laboratory studies by Stramski *et al*. (2002), where the acclimation to low temperature caused a significant increase in a^*_{ph} through reduced synthesis of Chl-*a*.

5. Conclusions

In this study, *Synechococcus* sp. was found to be an important phytoplankton group in the oceanic and coastal waters off Baja California, providing the main source of zeaxanthin in the southern region of the California Current. The contributions of size-fractionated biomass (μg C l^{-1}) to total phytoplankton were 46% for nano-microphytoplankton and 54% for picophytoplankton. The picophytoplankton fraction during January 2002 increased by ~36% compared with January 2001. Likewise, the mean diatom and dinoflagellate abundances off Baja California decreased 7 times and 68%, respectively, compared to the previous year for the same study area. We observed that a^*_{ph} tends to be high when zeaxanthin is present in elevated concentrations and with lower biomass and less photosynthetic pigments. A clear effect on the pelagic ecosystem was observed in January 2002 due to the waning of La Niña conditions. The higher microphytoplankton abundance located in the California Current was dominated by local and regional seasonal processes.

Acknowledgements

This study was supported by the IMECOCAL program and by the Mexican Council for Science and Technology (CONACyT project G-35326-T). We thank M. E. Sieracki for flow cytometry assistance at the Bigelow Laboratory for Ocean Sciences, and C. C. Trees for help with the HPLC pigment analysis. We also thank the crew of the *R/V Francisco de Ulloa* for their efficient help on board, J. M. Domínguez and F. J. Ponce for the drawings, and C. Harris for fine-tuning the English. The reviewers' comments were highly appreciated.

References

Álvarez-Borrego, J. and S. Álvarez-Borrego (1982): Temporal and spatial variability of temperature in two coastal lagoons. *CalCOFI Rep*., **XXIII**, 188–197.

Barocio-León, Ó. A., R. Millán-Núñez, E. Santamaría-del-Ángel, A. González-Silvera and C. C. Trees (2006): Spatial variability of phytoplankton absorption coefficients and pigments off Baja California during November 2002. *J. Oceanogr*., **62**, 873–885.

Barocio-León, Ó. A., R. Millán-Núñez, E. Santamaría-del-Ángel, A. González-Silvera, C. C. Trees and E. Orellana-Cepeda (2008): Bio-optical characteristics of a phytoplankton bloom event off Baja California peninsula (30–31°N). *Cont. Shelf Res*., **28**, 672–681.

Behrenfeld, M. J. and P. G. Falkowski (1997): A consumer's guide to phytoplankton primary productivity models. *Limnol. Oceanogr*., **42**(7), 1479–1491.

Blanchot, J., J. M. Andre, C. Navarrete, J. Neveux and M. H. Radenac (2001): Picoplankton in the equatorial Pacific: vertical distributions in the warm pool and in the high nutrient low chlorophyll conditions. *Deep-Sea Res. I*, **48**, 297–314.

Cleveland, J. S. and A. D. Wiedemann (1993): Quantifying absorption by aquatic particles: A multiple scattering correction for glass fiber filters. *Limnol. Oceanogr*., **38**(6), 1321–1327.

Durazo, R., G. Gaxiola-Castro, B. Lavaniegos-Espejo, R. Castro-Valdéz, J. Gómez Valdéz and A. Da. S. Mascarenhas, Jr. (2005): Oceanographic conditions west of the Baja California coast, 2002–2003: A weak El Niño and subarctic water enhancement. *Cienc. Mar*., **31**(3), 537–552.

Edler, L. (1979): Recommendations for marine biological studies in the Baltic Sea: Phytoplankton and chlorophyll. *Baltic Mar. Biol*., **5**, 1–38.

Gaxiola-Castro, G., R. Durazo, B. Lavaniegos, M. E. De La Cruz, E. Millán-Núñez, L. Soto Mardones and J. Cepeda-Morales (2008): Pelagic ecosystem response to interannual variability off Baja California. *Cienc. Mar*., **34**(2), 263–270.

Gin, K. Y., S. Zhang and Y. K. Lee (2003): Phytoplankton community structure in Singapore's coastal waters using HPLC pigment analysis and flow cytometry. *J. Plankton Res*., **25**(12), 1507–1519.

Goericke, R. R., J. Olson and A. Shalapyonok (2000): A novel niche for *Prochlorococcus* sp. in low-light suboxic environments in the Arabian Sea and the Eastern Tropical North Pacific. *Deep-Sea Res. I*, **47**, 1183–1205.

Hoepffner, N. and S. Sathyendranath (1991): Effect of pigment composition on absorption properties of phytoplankton. *Mar. Ecol. Prog. Ser*., **73**, 11–23.

Kiefer, D. A. and B. G. Mitchell (1983): A simple, steady state description of phytoplankton growth based on absorption cross section and quantum efficiency. *Limnol. Oceanogr*., **28**, 770–776.

Kishino, M., N. Takahashi, N. Okami and S. Ichimura (1985): Estimation of the spectral absorption coefficients of phytoplankton in the sea. *Bull. Mar. Sci*., **37**, 634–642.

Latasa, M. R., R. Bidigare, M. E. Ondrusek and M. C. Kennicutt (1996): HPLC analysis of Algal pigments: A comparison exercise among laboratories and recommendations for im-

proved analytical performance. *Mar. Chem.*, **51**, 315–324.
Licea, S., J. L. Moreno, H. Santoyo and G. Figueroa (1996): Dinoflageladas del Golfo de California. Universidad Autónoma de Baja California Sur, 165 pp.
Mantua, N. J., S. R. Hare, Y. Shang, J. M. Wallace and R. C. Francis (1997): A Pacific interdecadal climate oscillation with impacts on salmon production. *Bull. Am. Metereol. Soc.*, **78**, 1069–1079.
Millán-Núñez, E., M. E. Sieracki, R. Millán-Núñez, J. R. Lara-Lara, G. Gaxiola-Castro and C. C. Trees (2004): Specific absorption coefficient and phytoplankton biomass in the southern region of the California Current. *Deep-Sea Res. II*, **51**, 817–826.
Mitchell, B. G. (1990): Algorithms for determining the absorption coefficient of aquatic particulates using the quantitative filter technique (QFT). *Ocean Opt.*, **X** 1302, 137–148.
Morel, A. (1997): Consequences of a *Synechococcus* bloom upon the optical properties of oceanic (case 1) waters. *Limnol. Oceanogr.*, **42**, 1746–1754.
Moreno, J. L., S. Licea and H. Santoyo (1997): Diatomeas del Golfo de California. Universidad Autónoma de Baja California Sur, 273 pp.
National Centers for Environmental Prediction (2002): Climate Diagnosis Bulletin, March 2002. Climate Prediction Center, NOAA/NWS/NCEP, No. 02/3.
Nelson, N. B., B. B. Prezelin and R. R. Bidigare (1993): Phytoplankton light absorption and package effect in California coastal waters. *Mar. Ecol. Prog. Ser.*, **94**, 217–227.
Roden, G. I. (1971): Aspects of the transition zone in the northeastern Pacific. *J. Geophys. Res.*, **76**, 3462–3475.
Sathyendranath, S., A. Longhurst, C. M. Caverhill and T. Platt (1995): Regionally and seasonally differentiated primary production in the North Atlantic. *Deep-Sea Res. I*, **43**, 1773–1802.
Schwing, F. B., S. J. Bograd, C. A. Collin, G. Gaxiola-Castro, J. Garcia, R. Goericke, J. Gómez-Valdéz, J. A. Huyer, K. D. Hyrenbach, P. M. Koero, B. E. Lavaniegos, R. J. Lynn, A. W. Mantyla, M. D. Olman, W. T. Peterson, R. L. Smith, W. J. Sydeman, E. Venrick and P. A. Wheeler (2002): The state of the California Current, 2001–2002: will the California Current System keep its cool, or is El Niño looming? *CalCOFI Rep.*, **43**, 31–68.
Sosik, H. M. and B. G. Mitchell (1995): Light absorption by phytoplankton, photosynthetic pigments and detritus in the California Current System. *Deep-Sea Res. I*, **42**, 1717–1748.
Staehr, P. A., S. Markager and K. Sand-Jensen (2004): Pigment specific *in vivo* light absorption of phytoplankton from estuarine, coastal and oceanic waters. *Mar. Ecol. Prog. Ser.*, **275**, 115–228.
Stramski, D., A. Sciandra and H. Claustre (2002): Effects of temperature, nitrogen, and light limitation on the optical properties of the marine diatom *Thalassiosira pseudonana*. *Limnol. Oceanogr.*, **47**(2), 392–403.
Strathmann, R. R (1967): Estimating the organic carbon content of phytoplankton from cell volume or plasma. *Limnol. Oceanogr.*, **12**, 411–418.
Stuart, V., S. Sathyendranath, T. Platt and B. D. Irwin (1998): Pigments and species composition of natural phytoplankton populations: Effects on the absorption spectra. *J. Plankton Res.*, **20**, 187–217.
Utermöhl, H. (1958): Zur vervollkommnung der quantitativen phytoplankton-methodik. *Mitt. Int. Ver. Theor. Angew. Limnol.*, **5**, 567–596.
Verity, P. G., Ch. Y. Robertson, C. R. Tronzo, M. G. Andrews, J. R. Nelson and M. E. Sieracki (1992): Relationships between cell volume and the carbon and nitrogen content of marine photosynthetic nanoplankton. *Limnol. Oceanogr.*, **37**(7), 1434–1446.
Wolter, K. and M. S. Timlin (1998): Measuring the strength of ENSO: How does 1997/1998 rank? *Weather*, **53**, 315–324.
Wright, S. W., S. W. Jeffrey, R. F. Mantoura, C. A. Llewellyn, T. Bjornland, D. Repeta and N. Welschmeyer (1991): Improved HPLC method for the analysis of chlorophylls and carotenoids from marine phytoplankton. *Mar. Ecol. Prog. Ser.*, **77**, 183–196.
Wu, J., H. Hong, S. Shang, M. Dai and Z. Lee (2007): Variation of phytoplankton absorption coefficients in the northern South China Sea during spring and autumn. *Biogeosciences Discuss.*, **4**, 1555–1584.
Yentsch, C. S. and D. A. Phinney (1989): A bridge between ocean optics and microbial ecology. *Limnol. Oceanogr.*, **34**, 1694–1705.